Bioresource Technology 369 (2023) 128437

Contents lists available at ScienceDirect

Bioresource Technology

journal homepage: www.elsevier.com/locate/biortech

Intermittent ultrasound retains cellulases unlock for enhanced cellulosic ethanol with high-porosity biochar for dye adsorption using desirable rice mutant straw

Zhen Hu [a,b,c,1], Qian Li [a,1], Yuanyuan Chen [a], Tianqi Li [a], Youmei Wang [a], Ran Zhang [a], Hao Peng [a], Hailang Wang [a], Yanting Wang [a], Jingfeng Tang [b], Muhammad Nauman Aftab [d], Liangcai Peng [a,b,c,*]

[a] Biomass & Bioenergy Research Centre, College of Plant Science & Technology, Huazhong Agricultural University, Wuhan 430070, China
[b] Key Laboratory of Fermentation Engineering, National "111" Center for Cellular Regulation and Molecular Pharmaceutics, Cooperative Innovation Center of Industrial Fermentation, Hubei Key Laboratory of Industrial Microbiology, Hubei University of Technology, Wuhan 430068, China
[c] Biofuels Institute, School of Environment and Safety Engineering, Jiangsu University, Zhenjiang 212013, China
[d] Institute of Industrial Biotechnology, GC University, Lahore, Pakistan

HIGHLIGHTS

- A desirable recalcitrance-reduced lignocellulose was used from rice mutant straw.
- Optimal ultrasound pretreatment was specifically efficient for lignin extraction.
- Intermittent ultrasound is effective for more enzyme unlock and less lignin block.
- Highly-porous biochar was generated from undigestible residues for dye adsorption.
- A green-like biomass process is explored by a novel ultrasound treatment technology.

GRAPHICAL ABSTRACT

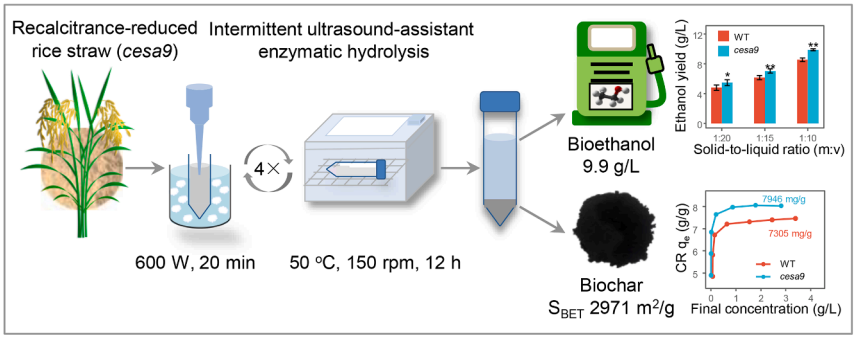

ARTICLE INFO

Keywords:
Bioethanol
Biochar
Ultrasound-assistant hydrolysis
Dye adsorption
Rice straw

ABSTRACT

In this study, optimal ultrasound pretreatment was performed with recalcitrance-reduced rice mutant straw to effectively extract lignin and hemicellulose for improved cellulose accessibility. Intermittent ultrasound-assistant enzymatic hydrolyses were followed to maintain more cellulases unlock and less cellulose surface block with lignin for raised hexose yield at 81 % (% cellulose) and bioethanol concentration at 9.9 g/L, which was higher than those of other mechanical pretreatments as previously conducted. Using all enzyme-undigestible lignocellulose residues, this work generated the biochar with the highest porosity (S_{BET} at 2971 m^2/g) among all biomass-based biochar obtained from previous studies. Furthermore, the biochar were respectively examined with high adsorption capacity for Congo red and methylene blue at 7946 mg/g and 861 mg/g. Therefore, this

* Corresponding author at: Biomass & Bioenergy Research Centre, College of Plant Science & Technology, Huazhong Agricultural University, Wuhan 430070, China.
E-mail address: lpeng@mail.hzau.edu.cn (L. Peng).
[1] Equal contributor.

https://doi.org/10.1016/j.biortech.2022.128437
Received 27 October 2022; Received in revised form 30 November 2022; Accepted 1 December 2022
Available online 5 December 2022

study has demonstrated a green-like process technology for high-yield bioethanol and high-porosity biochar with full biomass utilization by integrating optimal ultrasound pretreatment with intermittent ultrasound-assistant enzymatic hydrolyses of recalcitrance-reduced lignocellulose in crop straws.

1. Introduction

Biomass-based bioeconomy is regarded as a substitution of fossil-fuel-driven economy, while it relies on an efficient utilization of bio-resource (Liao et al., 2020). Although the co-production of bioethanol and biochemicals from lignocellulose residue is a feasible way for full biomass utilization (Kalyani et al., 2017), the inherent biomass recalcitrance determines a low saccharification and conversion efficiency (Himmel et al., 2007). Even though physical and chemical pretreatments are effective to break down the rigidity of biomass for high saccharification, the most pretreatment are energy-intensive and environmentally unfriendly (Cantero et al., 2019). Selection of recalcitrance-reduced lignocellulose along with mild and green-like biomass process has been considered as a promising solution for cost-effective production of biofuels and biomaterials (Wells et al., 2020).

Genetic improvement of plant cell wall is thought as a powerful solution to reduce the biomass recalcitrance, which is predominantly determined by cellulose crystallinity and lignin–carbohydrate complexes (Martínez, 2016; McCann and Carpita, 2015). In general, genetic manipulation of cellulose biosynthesis has been performed to effectively reduce cellulose recalcitrance for increased biomass enzymatic saccharification in bioenergy crops (Fan et al., 2017; Glass et al., 2015; Huang et al., 2019; Li et al., 2018). In particular, a natural site mutation of cellulose synthase (*CESA*) is identified for remarkably reduced cellulose crystallinity and polymerization in rice mutant (*Osfc16*) straw, leading to desirable cellulose nanofibrils generated for efficient conversion into fermentable sugar or nanomaterials (Li et al., 2017; Peng et al., 2022). As the natural rice mutant (*Osfc16*) shows a normal plant growth and improved lodging resistance to maintain high yields of grain and biomass, it provides a clue to select the desirable site mutants by performing CRISPR/Cas9 gene editing with cellulose synthase complexes.

Ultrasound pretreatment has emerged as a green-like technology to overcome biomass recalcitrant, as it has multiple advantages including high activation energy, short residence time, and efficient mass transfer for effective deconstruction of the lignocellulose without any chemical waste release (Choi et al., 2011). It is particularly effective for partial removal of hemicelluloses and lignin to improve cellulose accessibility (Mankar et al., 2021). However, while ultrasound pretreatment is conducted alone, it is limited for enhancement of sequential enzymatic saccharification (Easson et al., 2011). Hence, it remains to develop the novel ultrasound technology for further improving biomass enzymatic saccharification.

Biochar production from hydrolysis residue is a viable option for full biomass utilization (Kalyani et al., 2017). Because biochar is of stable structure, large pore volume, high specific surface area and active functional groups, it has been widely applied in environmental remediation such as agricultural soil improvement and industrial wastewater clearness (Pan et al., 2021). The adsorption performance of biochar depends on its physicochemical properties (Cheng et al., 2021). Taking advantage of the biodegradation and infiltrability of hyphae, a hierarchical porous carbon is generated with ultra-high specific surface area, large pore volume, abundant pores and advanced adsorption capacity from agricultural waste edible fungus slag (Cheng et al., 2019). Meanwhile, a nitrogen-doping of biochar generated from enzyme-undigested cellulose residue is also synthesized serving as the lithium-sulfur cathode that displays high discharge capacity and coulombic efficiency (Xu et al., 2020).

Rice is a staple food crop with large amounts of lignocellulose-rich straw convertible for biofuels and bioproduction (Bhattacharyya et al., 2019). In this study, the straw sample of rice site-mutant was collected with much recalcitrance-reduced lignocellulose residue by performing *OsCESA9* gene-editing. To find out a green-like pretreatment with desirable lignocellulose substrate, this study performed optimal ultrasound pretreatments with the rice straws of both mutant and its wild type, and further explored the ultrasound-assistance enzymatic hydrolyses of pretreated residues for integrative enhancement of biomass saccharification. Notably, to establish a full-chain of biomass process, this study collected all remaining enzyme-undigestible residues to generate highly-porous biochar, and detected much raised adsorption capacity with Conge red (CR) and methylene blue (MB) for potential dye remediation, providing a green-like strategy applicable for relatively low-cost biofuels and high-value bioproducts.

2. Material and methods

2.1. Collection of the cesa9 mutant generated by CRISPR/Cas9 gene-editing

The *cesa9* mutants were generated by using a precise base-replacement CRISPR/Cas9 system as described by Lu and Zhu (2017). The sgRNA targeting to the ZnF domain of *OsCESA9* was sought by the CRISPR-PLANT tool basing on the reference genome of *Oryza sativa L. cv. Nipponbare* (NPB). The sgRNA was cloned into the pCSGAPO1 vector and transformed into NPB calli via *Agrobacterium*-mediated transformation. The transgenic positive lines were screened by PCR amplifying using a *Cas9* gene specific primer. Genomic edits were checked by PCR amplifying and Sanger sequencing of the target regions. Potential off-target sites were identified by CRISPR-P program. Genomic regions neighboring six top-ranked potential off-target sites were checked by PCR amplifying and Sanger sequencing.

2.2. Rice biomass sample collection

The *cesa9* mutant and its wild type (WT/NPB) were planted in the field of Huazhong Agricultural University during 2019–2021. Ten rice plants were transplanted in each row, with row and column distances of 26 and 16 cm, respectively. After maturation, rice plants were harvested and their stems were dried at 60 °C. The stem samples were cut into pieces and then ground into powders. The biomass powders were screened pass a 40 mesh sieve (425 μm) and then stored in a dry container.

2.3. Soluble sugars and cell wall composition determination

Soluble sugars and wall polysaccharides were extracted and determined as described by Peng et al. (2000). Lignin content was measured by using the two-step acid hydrolysis method as described by Li et al. (2018) with minor modification. Biomass power was firstly extracted by benzene-ethanol solution for 4 h. After drying, the pellet was hydrolyzed by 67 % (v/v) H_2SO_4 at normal temperature for 1.5 h. The hydrolysate was then diluted to 2.88 % and followed by heating at 120 °C for 1 h. The ASL in supernatant was determined by UV spectroscopy ($\lambda = 205$ nm). The remaining residue was calcined at 575 ± 25 °C for 4 h. The AIL content was calculated as the weight of acid insoluble residues after subtracting ash. The sum of ASL and AIL represented the total lignin content.

2.4. Cellulose feature detection

The degree of polymerization (DP) of crude cellulose and crystalline cellulose substrates were measured by the viscometry method (Zhang et al., 2013). The crystalline celluloses were extracted by acetic acid–nitric acid–water (8: 1: 2, v/v/v), and the crude celluloses were extracted by 4 M KOH and 8 % (w/v) sodium chlorate (pH 4.5). Cellulose crystalline index (CrI) was measured by the X-ray diffraction (Li et al., 2018). Cellulose accessibility was detected by Congo red (CR) stain as previously described by Alam et al., (2019).

2.5. Ultrasound pretreatment and intermittent ultrasound treatment

The ultrasound pretreatment was carried out by using an ultrasonic processor (JY92-IIDN, China) at 22 kHz with an output power of 0–600 W for 0–80 min in an ice bath. The diameter of the amplitude-change pole was 6 mm and its top was placed at 0.5 cm below the liquid level. For intermittent treatment, ultrasound was conducted at 0, 12, 24 and 36 h during the enzymatic hydrolysis process with an output power of 600 W for 20 min each time.

2.6. Biomass enzymatic saccharification and yeast fermentation

Biomass enzymatic saccharification and final yeast fermentation were conducted as previously described by Li et al. (2018). The pretreated residues were incubated with 0.16 % (w/v) mixed-cellulases (Imperial Jade Biotechnology Co., China) with 1 % Tween-80 (v/v) co-supplied. The enzymatic hydrolysis was performed at 50 °C under 150 rpm shaken. The released hexose and pentose were measured by anthrone/H_2SO_4 and orcinol/HCl method, respectively. The activated yeast (Angel yeast Co., ltd., China) was inoculated into the enzymatic hydrolysates. The fermentation reaction was performed at 37 °C for 48 h. The fermentation solution was distilled for the determination of ethanol content. The ethanol content was measured by the $K_2Cr_2O_7$ method.

2.7. Enzyme concentration assay

During enzymatic hydrolysis, the supernatant was collected after centrifugation at 12,000 *g* for 10 min. SDS-PAGE analysis was carried out as previously described by Li et al. (2017). The enzyme concentration was diluted by 20 times before loading. The Bradford method was performed for quantitative assay of total proteins as previously described by Madadi et al. (2021). The enzyme concentration was calculated based on the curves established by the standard enzyme solution at various concentrations.

2.8. Biochar preparation

The raw materials and enzyme-undigestible residues were firstly carbonized at 400 °C for 3 h in N_2 atmosphere. After cooling to 25 °C, carbonized powders (1 g) were mixed with 4 g KOH and fully grounded. The solid mixtures were further heated at 800 °C for 3 h in N_2 atmosphere. The heading rate and cooling rate for two heating processes were 5 °C/min and 10 °C/min, respectively. The carbon residues were washed with 1 M HCl aqueous solution for 6 h to neutralize KOH, and finally washed with deionized water. The carbon sample was treated by ultrasound in a sonicator for 6 h and dried at 60 °C.

2.9. CR and MB adsorption measurements

CR solution (20 g/L) was prepared using 0.3 M phosphate buffer as the solvent, while MB solution (1 g/L) was prepared using ultra-pure water as the solvent. About 20 mg biochar and 20 mL CR or MB solution were supplemented in 50 mL tubes. Adsorption experiments were carried out at 25 °C with 150 rpm shaken for 6 h. The initial concentrations of CR solution were 5, 6, 7, 8, 9, 10 and 11 g/L, and those of MB solution were 0.4, 0.5, 0.6, 0.7, 0.8, 0.9 and 1.0 g/L. After adsorption, the samples were centrifuged at 12,000 *g* for 10 min, and the residual CR and MB concentration in the supernatant were determined by a UV–vis spectrometer at 498 nm and 668 nm, respectively. The maximum dye adsorption capacity was calculated using monolayer Langmuir adsorption model. The adsorption rates were evaluated with 5 g/L CR solution and 1 g/L MB solution at 25 °C for 0 – 60 min.

2.10. AFM, FTIR, SEM, BET and XPS characterization

Tissue section of rice stem with 80 μm thick was applied for *in situ* atomic force microscopy (AFM) observation. Innermost surface of the parenchyma secondary cell wall was selected for site observation. The Agilent multipurpose AFM scanner with open-loop was applied for all recognition imaging. The PicoPlus Molecular Imaging system together with a PicoScan 3000 Controller was utilized for AFM quantitative measurement. Ten random zoom-in areas and 100 data points were collected for statistical analyses. Fourier transform infrared (FTIR) spectroscopy was performed using a PerkinElmer spectrophotometer (Nicolet Nexus 470, USA) equipped with diamondegermanium ATR single reflection crystal. The morphology of the biomass samples was characterized by scanning electron microscopy (Hitachi SU8020). The electronic binding energy of biochar was obtained by using X-ray photoelectron spectroscopy on the ESCALab 250Xi (Thermo Scientific) instrument. The specific surface area and pore size of biochar were detected using the ASAP2460 (Micromeritics) analyzer at 77.3 K.

2.11. Statistical analysis

Student's *t*-test and Analyses of Variance (ANOVA) were performed using the SPSS 23 software (Inc., Chicago, IL). The plotting was conducted using ggplot2 package installed in R software (V 4.1.2).

3. Results and discussion

3.1. Altered cell wall composition and cellulose nanofibrils in the desirable rice mutant straw

As described above, this study initially collected a desirable rice mutant sample by performing site mutation of OsCESA9 protein, which is characterized as the essential isoform of cellulose synthase complexes for cellulose biosynthesis of plant secondary cell walls (Tanaka et al., 2003). The *cesa9* mutant was of decreased plant height and extension force, but its biomass yield was significantly increased at $p < 0.05$ level, compared to its wild type/WT (see supplementary materials). Using mature rice straw, this study examined much reduced cellulose level and raised lignin content with more soluble sugar accumulation relative to the WT (Fig. 1 A), which explained why the *cesa9* mutant had relatively higher total biomass yield. Furthermore, this study examined significantly reduced DP values of crude cellulose and crystalline cellulose substrates by 14.7 % and 31.6 % in the *cesa9* mutant, respectively (Fig. 1 B). Meanwhile, the cellulose CrI was also reduced by 13.2 % in the mutant (Fig. 1 C). By means of our-recently-established AFM approach (Peng et al., 2022; Zhang et al., 2020a), cellulose microfibrils assembly in the de-lignin plant cell walls were observed *in situ* (see supplementary materials), and the average length of cellulose nanofibrils were then measured by scaling the distance of two amorphous/non-crystalline cellulose chains on the surfaces of cellulose microfibrils (Fig. 1 D). As a comparison, the WT sample showed the average cellulose nanofibers length at 125 nm, whereas the *cesa9* mutant was at 97.7 nm, being consistent with much reduced cellulose CrI and DP values examined in the mutant. Hence, the length-reduced cellulose nanofibrils should be accountable for relatively raised amorphous cellulose chain assembly in the *cesa9* mutant.

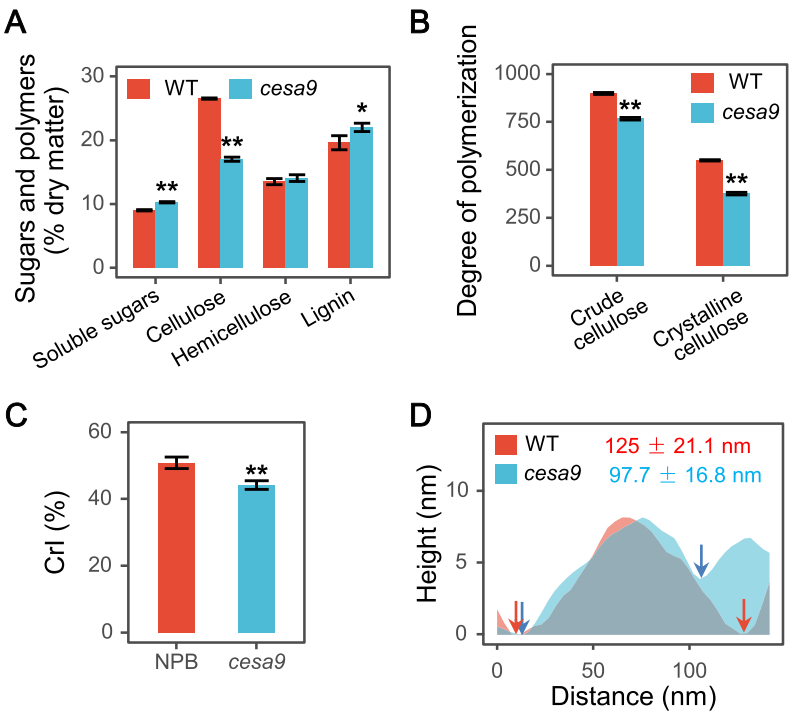

Fig. 1. Cell wall composition and cellulose features of rice mature straws in the *cesa9* mutant and WT. (A) Soluble sugars and wall polymer levels; (B) Degree of polymerization (DP) of crude cellulose and crystalline cellulose substrates; (C) Cellulose crystalline index (CrI); (D) Evaluation of the average distance between two amorphous/non-crystalline cellulose chains on the surfaces of cellulose microfibrils accountable for average length of cellulose nanofibrils by randomly-selected 100 samples, the data as mean ± SD (n = 100). The arrows indicate the amorphous regions. * and ** represented significant difference at $p < 0.05$ and 0.01 (n = 3), respectively.

3.2. Ultrasound pretreatment followed with intermittent ultrasound for enhanced biomass enzymatic saccharification

Because the amorphous cellulose chains have been considered as the breakpoints for initiating and completing cellulose hydrolysis into soluble sugars (Martínez, 2016), this study determined biomass saccharification of the *cesa9* mutant by measuring hexose yield (% cellulose) released from lignocellulose enzymatic hydrolysis (Fig. 2). Without any pretreatment, the mutant displayed much higher hexoses yields than those of the WT (Fig. 2A), consistent with recalcitrance-reduced lignocellulose features in the mutant such as reduced cellulose DP and CrI, and raised amorphous cellulose chain as described

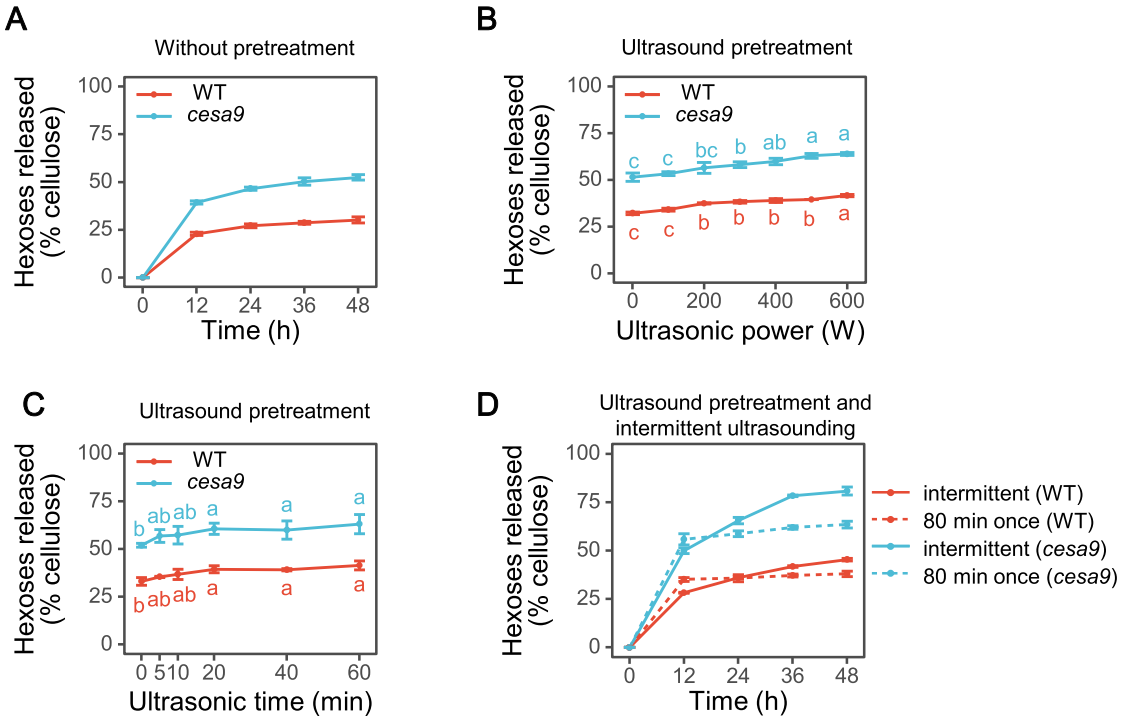

Fig. 2. Biomass saccharification of rice mature straws in the *cesa9* mutant and WT under optimal ultrasound pretreatments followed with intermittent ultrasound-assistance enzymatic hydrolyses. (A) Hexose yields (% cellulose) released from time-course enzymatic hydrolysis without pretreatment; (B and C) Hexoses yields (% cellulose) released from enzymatic hydrolyses under ultrasound pretreatments at various powers for 20 min and with 600 W under a time course; (D) Hexoses yields released from enzymatic hydrolyses under ultrasound pretreatment and intermittent ultrasound-assistance enzymatic hydrolyses. The intermittent ultrasounding was conducted at 0, 12, 24 and 36 h.

above. As ultrasound is a typically green-like (nonchemical) pretreatment, this study explored different conditions (power, incubation time) of ultrasound pretreatments with rice straws (Fig. 2B-C). As a result, the optimal ultrasound pretreatment (600 W, 20 min) could lead to hexoses yields raised by 22 %-25 %, compared to the control (without pretreatment). Notably, as the optimal ultrasound pretreatment respectively caused<53 % and 32 % cellulose hydrolyses into fermentable hexoses in the mutant and WT, this study further performed intermittent ultrasound during the enzymatic hydrolyses of pretreated lignocellulose residues, and determined their cellulose hydrolyses at 81 % and 45 % (Fig. 2D), suggesting that the intermittent ultrasound-assistant enzymatic hydrolyses should play an active role for enhancing enzymatic saccharification. As a further comparison with the previous reports from other physical/mechanical pretreatments conducted with diverse biomass resources, this study achieved the highest hexoses yields in the desirable mutant straw (da Silva et al., 2010; Hideno et al., 2009; Ivetic et al., 2017; Yu et al., 2009; Zakaria et al., 2014; Zakaria et al., 2014; Zhang et al., 2020b). In addition, the mutant remained consistently higher enzymatic saccharification than that of the WT, which should be mainly due to much recalcitrance-reduced lignocellulose in the mutant as examined above. Hence, this study has sorted out the synergistic enhancements on biomass saccharification by integrating the genetic-modified cellulose substrate, optimal ultrasound pretreatment and intermittent ultrasound-assistance enzymatic hydrolysis.

3.3. Raised ethanol fermentation under ultrasound pretreatment and intermittent ultrasound treatment

Based on a previously-established approach (Li et al., 2018), this study conducted a classic yeast fermentation for bioethanol production by using all hexoses released from enzymatic hydrolyses of pretreated lignocellulose residues (Fig. 3). To achieve high concentration/yield of bioethanol, this study loaded three solid–liquid (1:20, 1:15, 1:10) ratios of lignocellulose substrates into enzymatic hydrolyses with intermittent ultrasound treatment were performed. In general, both rice mutant and WT samples showed an increasing hexose yield (g/L) released from enzymatic hydrolysis, while the solid–liquid ratio was rising from 1:20 to 1:10 (Fig. 3A). However, on the basis of hexose yield against cellulose level (% cellulose), three solid–liquid ratios of lignocellulose substrates showed a slightly altered cellulose digestion rate (Fig. 3B). Notably, the following intermittent ultrasound treatment could remarkably enhance both hexose yields (g/L, % cellulose) in all enzymatic hydrolyses performed in the mutant and WT samples, compared to their controls (without intermittent ultrasound). For instance, under the intermittent ultrasound treatment, the mutant sample (1:10 loading) produced the hexose yield at 22 g/L or 70 % (% cellulose), whereas the hexose yield of 17.5 g/L or 39 % (% cellulose) was only obtained from the controls. Meanwhile, this study examined that the mutant produced much more hexoses yields than those of the WT, in particular from the intermittent ultrasound treatment, which confirmed a consistently higher biomass enzymatic saccharification in the mutant.

As a consequence, this study achieved the highest bioethanol yields at 8.5 g/L and 9.9 g/L in the WT and mutant samples (Fig. 3C), due to their relatively higher hexoses yields than those of other samples as just examined. In addition, this work calculated sugar-ethanol conversion rate, and all samples showed a close conversion rate even though under the intermittent ultrasound treatment (Fig. 3D), suggesting that the intermittent ultrasound treatment should not produce extra toxic compounds that inhibit yeast fermentation. Taken together, this study has demonstrated a novel and green-like technology for enhancing biomass enzymatic saccharification and bioethanol production by using intermittent ultrasound-assistant enzymatic hydrolysis in the desirable lignocellulose substrate.

3.4. Distinct wall polymer extraction from ultrasound pretreatment

To understand why the ultrasound process led to much enhanced biomass enzymatic saccharification for bioethanol production, this study examined wall polymer compositions and interlinkages in the ultrasound pretreated lignocellulose residues (Fig. 4). Compared to their raw materials, both *cesa9* mutant and WT samples showed much reduced lignin levels with relatively less hemicelluloses, leading to significantly raised cellulose contents in the pretreated residue (Fig. 4A-B). The results suggest that the ultrasound pretreatment should lead to a major lignin extraction with small amount of hemicellulose co-extraction, being similar to classic alkali pretreatments examined

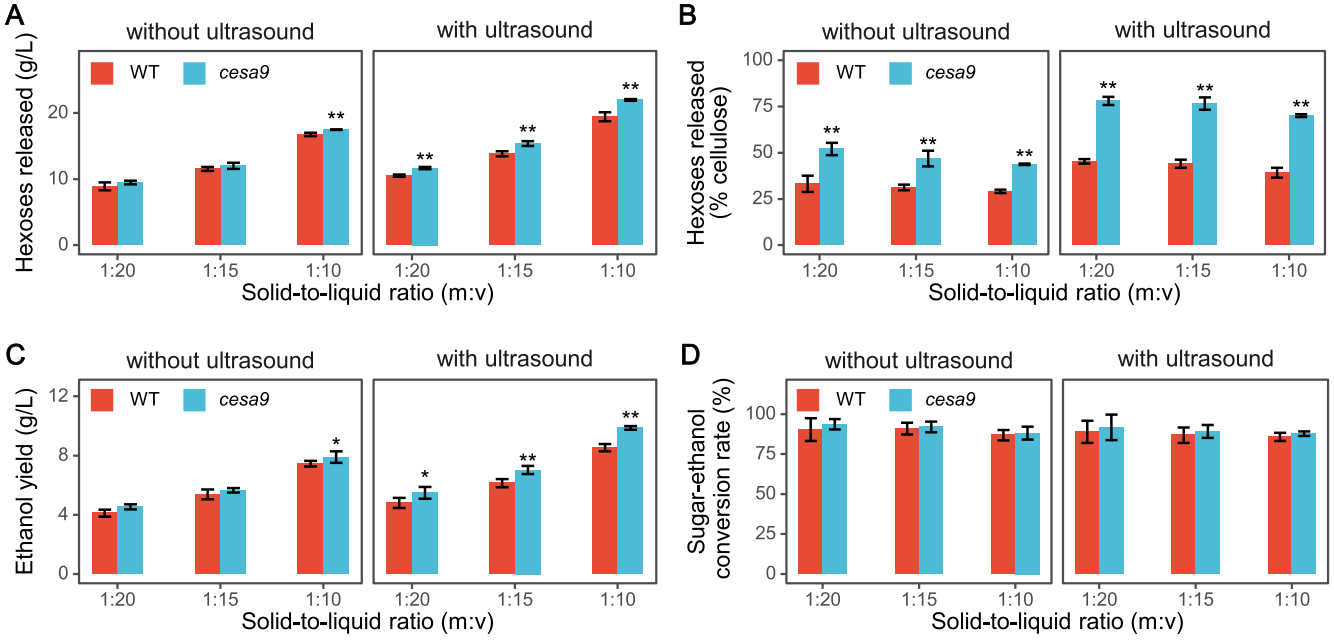

Fig. 3. Biomass saccharification and bioethanol fermentation by loading rice mature straws of the *cesa9* mutant and WT at three solid–liquid ratios with intermittent ultrasound-assistance enzymatic hydrolyses. (A and B) Total hexoses yields (g/L, % cellulose) released from both soluble sugars and enzymatic hydrolyses; (C and D) Bioethanol concentration (g/L) and sugar-ethanol conversion rates. * and ** represented significant difference at $p < 0.05$ and 0.01 level (n = 3), respectively.

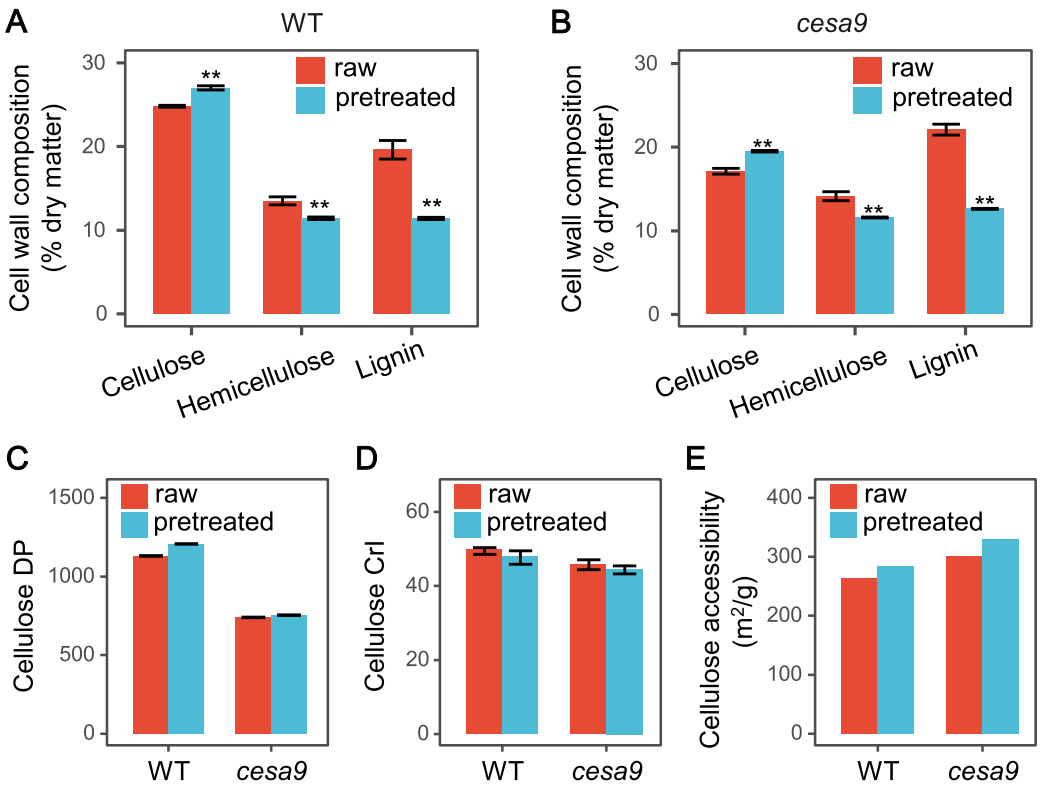

Fig. 4. Altered wall polymer levels in the mutant and WT from optimal ultrasound pretreatment. (A and B) Cell wall composition; (C and D) Cellulose DP and CrI; (E) Cellulose accessibility by CR staining assay. * and ** represented significant difference at $p < 0.05$ and 0.01 level (n = 3), respectively.

before (Si et al., 2015). However, unlike alkali pretreatment, the ultrasound pretreatment could not significantly improve cellulose features such as CrI and DP values (Fig. 4C, D), which may explain why the optimal ultrasound pretreatment could not cause a near-complete biomass enzymatic saccharification even though for the recalcitrance-reduced rice mutant. Furthermore, despite the lignin and hemicellulose extraction could increase cellulose accessibility in the pretreated residues, the *cesa9* mutant remained relatively higher cellulose accessibility than that of the WT (Fig. 4E), which should be accounting for higher biomass saccharification and bioethanol production achieved in the mutant.

3.5. Consistent enzyme unlocking by intermittent ultrasound assistance

Provided that the optimal ultrasound pretreatment is limited for near-complete biomass enzymatic saccharification, this study has consequently performed intermittent ultrasound-assistant enzymatic hydrolysis to further raise higher hexose and ethanol production as described above. To understand the mechanism of intermittent ultrasound-assistant enzymatic hydrolysis, this study first detected that the long-time ultrasound treatments had little impact on enzymatic hydrolyses of pretreated lignocellulose residues in both mutant and WT samples, indicating the enzyme activity was not affected by ultrasound treatment (Fig. 5A). However, during the intermittent ultrasound-assistant enzymatic hydrolyses, relatively more enzymes (commercial mixed-cellulases) occurred in the supernatants from SDS-PAGE profiling compared to the controls (without/before intermittent ultrasound) in the mutant and WT samples (Fig. 5B), which were confirmed by protein assay of the supernatants (Fig. 5C). The results thus reveal that the intermittent ultrasound treatment should be effective to protect the cellulases enzymes to be unlocked, possibly by maintaining enzyme disassociation with lignin. By contrast, while raw materials of rice straws were applied for direct enzymatic hydrolyses in the mutant and WT (without ultrasound pretreatment), a reducing enzyme concentration in the supernatants was determined (see supplementary materials), which should be mainly due to either a rich lignin deposition in raw materials or the soluble lignin-hemicellulose complex that tightly interact with cellulases (Cantero et al., 2019). Furthermore, a relatively higher cellulose accessibility was determined during the intermittent ultrasound-assistant enzymatic hydrolyses in the mutant and WT samples (Fig. 5D), confirming that the intermittent ultrasound should also maintain lignin disassociation with cellulose microfibrils or cellulases enzymes during enzymatic hydrolysis performed. Hence, much raised rough surfaces of lignocellulose residues were observed after ultrasound-assistant enzymatic hydrolyses in both mutant and WT samples (see supplementary materials), providing an evidence about much enhanced biomass saccharification from the intermittent ultrasound-assistance hydrolyses conducted in this study. However, it remains to further explore how the intermittent ultrasound is effective to maintain lignin disassociation in the further study.

3.6. Porous biochar generated from enzyme-undigestible lignocelluloses for chemical adsorption

As described above, intermittent ultrasound-assistant enzymatic hydrolysis has provided a green-like approach for biomass saccharification and bioethanol production, but both mutant and WT samples remained enzyme-undigestible residues rich at lignin (see supplementary materials). By performing classic thermochemical conversion, this study generated biochar samples using all enzyme-undigestible lignocellulose residues in both mutant and WT. As a comparison with ones from raw materials of rice straws, the biochar samples from enzyme-undigestible residues showed consistently higher specific surface area and pore volume (Fig. 6 A, B). Meanwhile, the biochar generated from the mutant enzyme-undigestible residue remained higher specific surface area and pore volume than those of the WT by 8.6 % and 9.6 %, and its specific surface area and pore volume respectively reached to 2970.7 m^2/g and 2.4 cm^3/g, which should be either the highest surface area or

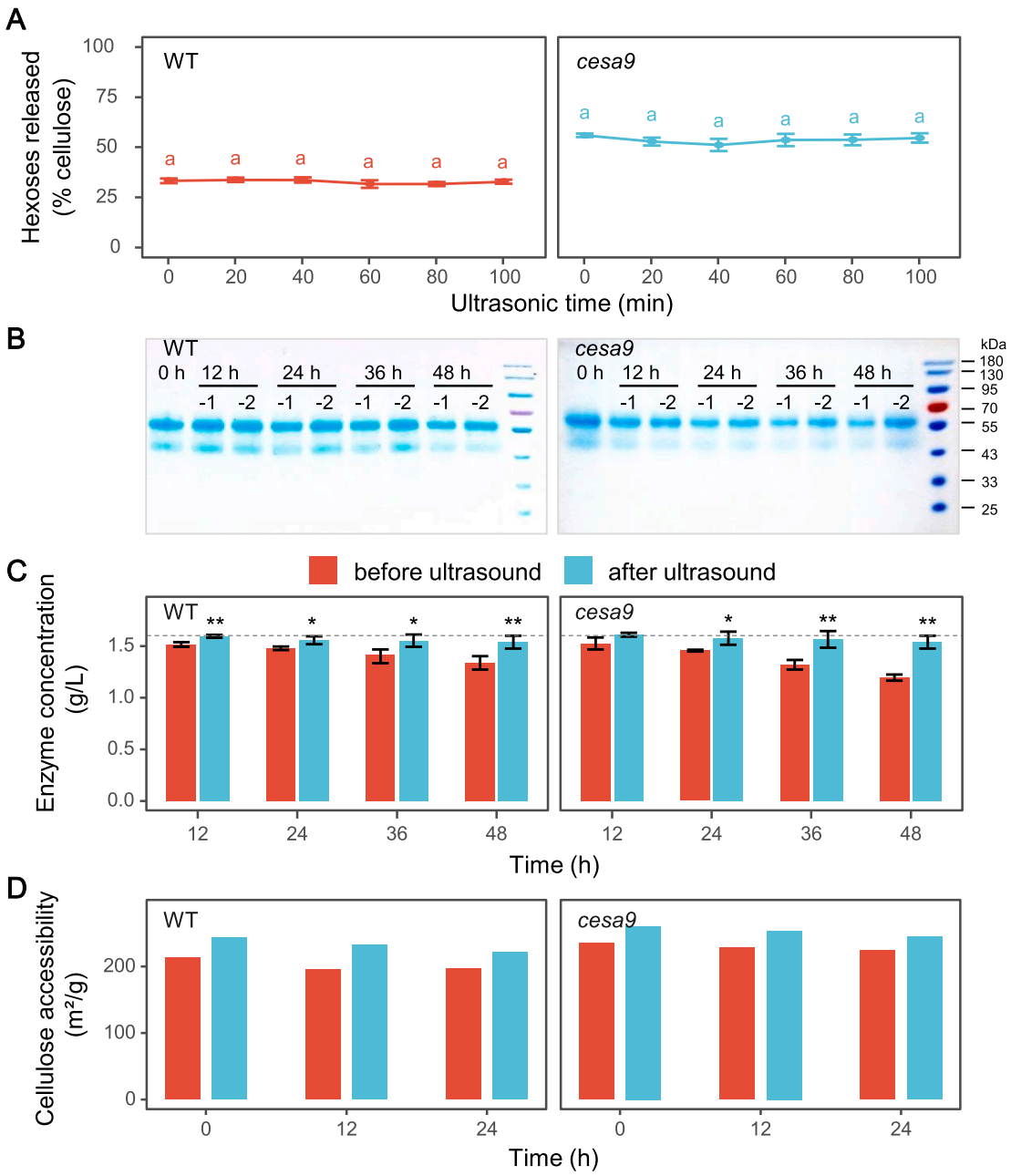

Fig. 5. Intermittent ultrasound-assistant enzymatic hydrolyses of lignocellulose residues in the *cesa9* mutant and WT. (A) Effect of ultrasound treatment on the activity of enzyme. The ultrasound-treated enzyme solution was applied for enzymatic hydrolysis of rice straw. Enzymatic activity was not decreased after ultrasound treatment at 600 W for 0–100 min; (B) SDS-PAGE profiling of enzymatic hydrolysates with the enzyme concentration diluted 20 times before loading; (C) Enzyme concentration in the supernatant as highlighted in (B) detected by Bradford assay; (D) Cellulose accessibility of solid substrates by Congo red staining assay. * and ** represented significant difference at $p < 0.05$ and 0.01 level ($n = 3$), respectively. (For interpretation of the references to colour in this figure legend, the reader is referred to the web version of this article.)

the second high pore volume among all biochar samples as previously obtained from diverse biomass resources (Jiang et al., 2022; Kong et al., 2014; Kumar and Jena, 2016; Mbarki et al., 2022; Prusov et al., 2021; Wang et al., 2022; Wu et al., 2020; Yu et al., 2019; Zheng et al., 2021). Furthermore, XPS assay showed major C and O elements occurred in all biochar samples (see supplementary materials), confirming a typical biochar generated in this study (Cheng et al., 2019).

To test the biochar function, this study performed its adsorption capacity with two organic chemicals (CR and MB), which are two typical wastes of dye industry (Kumar and Jena, 2016; Yu et al., 2019). As a comparison, the biochar of mutant samples showed consistently higher CR and MB adsorption capacities than those of the WT (Fig. 6 C, D), consistent with their distinct specific surface areas and pore volumes as examined. In particular, the biochar generated from mutant's enzyme-undigestible residue was of the highest CR adsorption capacity at 7946 mg/g and the third high MB adsorption at 861 mg/g among all biochar samples as previously detected (Jiang et al., 2022; Kong et al., 2014; Kumar and Jena, 2016; Mbarki et al., 2022; Prusov et al., 2021; Wang et al., 2022; Wu et al., 2020; Yu et al., 2019; Zheng et al., 2021). Furthermore, a time-course of CR and MB adsorption was conducted and all biochar samples showed a fast adsorption to reach the maximum within 20 min (see supplementary materials), consistent with the previous report about biochar adsorption (Cheng et al., 2019). Therefore, the enzyme-undigestible residues of rice mutant straw are convertible to

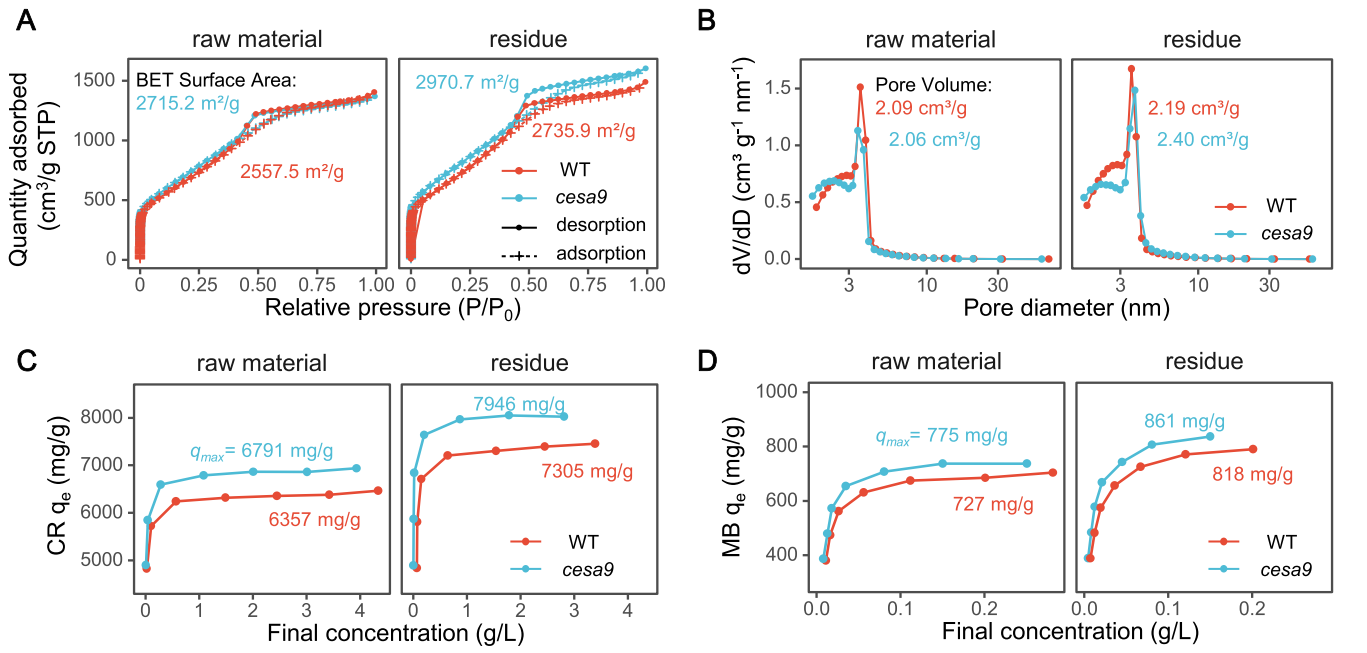

Fig. 6. Porous biochar samples generated from raw materials and enzyme-undigestible residues after intermittent ultrasound-assistant enzymatic hydrolyses of rice mutant and WT. (A and B) N_2 adsorption–desorption isotherms and pore-size distribution of biochar samples; (C and D) Adsorption isotherms of biochar samples for Congo red and methylene blue adsorption at 25 °C; ** As significant difference between the mutant and WT by *t*-test at $p < 0.01$ level (n = 3), respectively. (For interpretation of the references to colour in this figure legend, the reader is referred to the web version of this article.)

generate typically highly-porous biochar for efficient adsorption with dye chemicals.

4. Conclusions

By collecting recalcitrance-reduced lignocellulose substrate of rice mutant straw, this study performed optimal ultrasound pretreatment followed with intermittent ultrasound-assistant enzymatic hydrolysis for remarkably raised hexose yield at 81 % (% cellulose), leading to the higher bioethanol yield achieved at 9.9 g/L. Using all enzyme-undigestible lignocellulose residues, a typically porous biochar was generated with much high adsorption capacities for two dye (CR, MB) chemicals. Therefore, this study has demonstrated a green-like strategy for high-yield of bioethanol and high-porosity biochar with full biomass utilization by integrating optimal ultrasound pretreatment with intermittent ultrasound-assistant enzymatic hydrolyses of desirable lignocelluloses in bioenergy crops.

CRediT authorship contribution statement

Zhen Hu: Methodology, Formal analysis, Investigation, Writing – original draft. **Qian Li:** Methodology, Formal analysis, Investigation. **Yuanyuan Chen:** Investigation, Validation. **Tianqi Li:** Investigation, Formal analysis. **Youmei Wang:** Validation, Writing – review & editing. **Ran Zhang:** Validation, Writing – review & editing. **Hao Peng:** Investigation, Validation. **Hailang Wang:** Validation, Formal analysis. **Yanting Wang:** Supervision, Writing – review & editing. **Jingfeng Tang:** Writing – review & editing, Funding acquisition. **Muhammad Nauman Aftab:** Methodology, Writing – review & editing. **Liangcai Peng:** Methodology, Supervision, Writing – review & editing, Funding acquisition.

Declaration of Competing Interest

The authors declare that they have no known competing financial interests or personal relationships that could have appeared to influence the work reported in this paper.

Data availability

Data will be made available on request.

Acknowledgments

This work was in part supported by the National Natural Science Foundation of China (32101701, 32170268, 32100214, 52170081) and National 111 Project of Ministry of Education of China (BP0820035, D17009).

Appendix A. Supplementary data

Supplementary data to this article can be found online at https://doi.org/10.1016/j.biortech.2022.128437.

References

Alam, A., Zhang, R., Liu, P., Huang, J., Wang, Y., Hu, Z., Madadi, M., Sun, D., Hu, R., Ragauskas, A.J., Tu, Y., Peng, L., 2019. A finalized determinant for complete lignocellulose enzymatic saccharification potential to maximize bioethanol production in bioenergy *Miscanthus*. Biotechnol. Biofuels 12, 99.

Bhattacharyya, P., Bhaduri, D., Adak, T., Munda, S., Satapathy, B.S., Dash, P.K., Padhy, S. R., Pattanayak, A., Routray, S., Chakraborti, M., Baig, M.J., Mukherjee, A.K., Nayak, A.K., Pathak, H., 2019. Characterization of rice straw from major cultivars for best alternative industrial uses to cutoff the menace of straw burning. Ind. Crop. Prod. 143, 111919.

Cantero, D., Jara, R., Navarrete, A., Pelaz, L., Queiroz, J., Rodríguez-Rojo, S., Cocero, M. J., 2019. Pretreatment processes of biomass for biorefineries: current status and prospects. Annu. Rev. Chem. Biomol. Eng. 10, 289–310.

Cheng, J., Gu, J.J., Tao, W., Wang, P., Liu, L., Wang, C.Y., Li, Y.K., Feng, X.H., Qiu, G.H., Cao, F.F., 2019. Edible fungus slag derived nitrogen-doped hierarchical porous carbon as a high-performance adsorbent for rapid removal of organic pollutants from water. Bioresour. Technol. 294, 122149.

Cheng, N., Wang, B., Wu, P., Lee, X., Xing, Y., Chen, M., Gao, B., 2021. Adsorption of emerging contaminants from water and wastewater by modified biochar: A review. Environ. Pollut. 273, 116448.

Choi, J.A., Hwang, J.H., Dempsey, B.A., Abou-Shanab, R.A.I., Min, B., Song, H., Lee, D.S., Kim, J.R., Cho, Y., Hong, S., Jeon, B.H., 2011. Enhancement of fermentative bioenergy (ethanol/hydrogen) production using ultrasonication of *Scenedesmus obliquus* YSW15 cultivated in swine wastewater effluent. Energ. Environ. Sci. 4, 3513–3520.

da Silva, A.S.A., Inoue, H., Endo, T., Yano, S., Bon, E.P.S., 2010. Milling pretreatment of sugarcane bagasse and straw for enzymatic hydrolysis and ethanol fermentation. Bioresour. Technol. 101, 7402–7409.
Easson, M.W., Condon, B., Dien, B.S., Iten, L., Slopek, R., Yoshioka-Tarver, M., Lambert, A., Smith, J., 2011. The application of ultrasound in the enzymatic hydrolysis of switchgrass. Appl. Biochem. Biotechnol. 165, 1322–1331.
Fan, C., Feng, S., Huang, J., Wang, Y., Wu, L., Li, X., Wang, L., Tu, Y., Xia, T., Li, J., Cai, X., Peng, L., 2017. *AtCesA8*-driven *OsSUS3* expression leads to largely enhanced biomass saccharification and lodging resistance by distinctively altering lignocellulose features in rice. Biotechnol. Biofuels 10, 221.
Glass, M., Barkwill, S., Unda, F., Dmansfield, S.D., 2015. Endo-β-1,4-glucanases impact plant cell wall development by influencing cellulose crystallization. J. Integr. Plant Biol. 57, 396–410.
Hideno, A., Inoue, H., Tsukahara, K., Fujimoto, S., Minowa, T., Inoue, S., Endo, T., Sawayama, S., 2009. Wet disk milling pretreatment without sulfuric acid for enzymatic hydrolysis of rice straw. Bioresour. Technol. 100, 2706–2711.
Himmel, M.E., Ding, S.Y., Johnson, D.K., Adney, W.S., Nimlos, M.R., Brady, J.W., Foust, T.D., 2007. Biomass recalcitrance: engineering plants and enzymes for biofuels production. Science 315, 804–807.
Huang, J., Xia, T., Li, G., Li, X., Li, Y., Wang, Y., Chen, Y., Xie, G., Bai, F.W., Peng, L., Wang, L., 2019. Overproduction of native endo-β-1,4-glucanases leads to largely enhanced biomass saccharification and bioethanol production by specific modification of cellulose features in transgenic rice. Biotechnol. Biofuels 12, 11.
Ivetic, D.Z., Omorjan, R.P., Dordevic, T.R., Antov, M.G., 2017. The impact of ultrasound pretreatment on the enzymatic hydrolysis of cellulose from sugar beet shreds: modeling of the experimental results. Environ. Prog. Sustain. Energy 36, 1164–1172.
Jiang, F., Gao, D., Hu, S., Wang, Y., Zhang, Y., Huang, X., Zhao, H., Wu, C., Li, J., Ding, Y., Liu, K., 2022. High-pressure carbon dioxide-hydrothermal enhance yield and methylene blue adsorption performance of banana pseudo-stem activated carbon. Bioresour. Technol. 354, 127137.
Kalyani, D.C., Fakin, T., Horn, S.J., Tschentscher, R., 2017. Valorisation of woody biomass by combining enzymatic saccharification and pyrolysis. Green Chem. 19, 3302–3312.
Kong, J., Yue, Q., Gao, B., Li, Q., Wang, Y., Ngo, H.H., Guo, W., 2014. Porous structure and adsorptive properties of hide waste activated carbons prepared via potassium silicate activation. J. Anal. Appl. Pyrol. 109, 311–314.
Kumar, A., Jena, H.M., 2016. Removal of methylene blue and phenol onto prepared activated carbon from Fox nutshell by chemical activation in batch and fixed-bed column. J. Clean. Prod. 137, 1246–1259.
Li, Y., Liu, P., Huang, J., Zhang, R., Hu, Z., Feng, S., Wang, Y., Wang, L., Xia, T., Peng, L., 2018. Mild chemical pretreatments are sufficient for bioethanol production in transgenic rice straws overproducing glucosidase. Green Chem. 20, 2047–2056.
Li, F., Xie, G., Huang, J., Zhang, R., Li, Y., Zhang, M., Wang, Y., Li, A., Li, X., Xia, T., Qu, C., Hu, F., Ragauskas, A.J., Peng, L., 2017. OsCESA9 conserved-site mutation leads to largely enhanced plant lodging resistance and biomass enzymatic saccharification by reducing cellulose DP and crystallinity in rice. Plant Biotechnol. J. 15, 1093–1104.
Liao, Y., Koelewijn, S.F., Van den Bossche, G., Van Aelst, J., Van den Bosch, S., Renders, T., Navare, K., Nicolai, T., Van Aelst, K., Maesen, M., Matsushima, H., Thevelein, J.M., Van Acker, K., Lagrain, B., Verboekend, D., Sels, B.F., 2020. A sustainable wood biorefinery for low-carbon footprint chemicals production. Science 367, 1385–1390.
Lu, Y., Zhu, J.K., 2017. Precise editing of a target base in the rice genome using a modified CRISPR/Cas9 system. Mol. Plant 10, 523–525.
Madadi, M., Wang, Y.M., Xu, C.B., Liu, P., Wang, Y.T., Xia, T., Tu, Y.Y., Lin, X.C., Song, B., Yang, X., Zhu, W.B., Duanmu, D.Q., Tang, S.W., Peng, L.C., 2021. Using *Amaranthus* green proteins as universal biosurfactant and biosorbent for effective enzymatic degradation of diverse lignocellulose residues and efficient multiple trace metals remediation of farming lands. J. Hazard. Mater. 406, 124727.
Mankar, A.R., Pandey, A., Modak, A., Pant, K.K., 2021. Pretreatment of lignocellulosic biomass: A review on recent advances. Bioresour. Technol. 334, 125235.
Martínez, A.T., 2016. How to break down crystalline cellulose. Science 352, 1050–1051.
Mbarki, F., Selmi, T., Kesraoui, A., Seffen, M., 2022. Low-cost activated carbon preparation from Corn stigmata fibers chemically activated using H_3PO_4, $ZnCl_2$ and KOH: Study of methylene blue adsorption, stochastic isotherm and fractal kinetic. Ind. Crop. Prod. 178, 114546.
McCann, M.C., Carpita, N.C., 2015. Biomass recalcitrance: a multi-scale, multi-factor, and conversion-specific property. J. Exp. Bot. 66, 4109–4118.
Pan, X., Gu, Z., Chen, W., Li, Q., 2021. Preparation of biochar and biochar composites and their application in a Fenton-like process for wastewater decontamination: A review. Sci. Total Environ. 754, 142104.
Peng, L., Hocart, C.H., Redmond, J.W., Williamson, R.E., 2000. Fractionation of carbohydrates in *Arabidopsis* root cell walls shows that three radial swelling loci are specifically involved in cellulose production. Planta 211, 406–414.
Peng, H., Zhao, W., Liu, J., Liu, P., Yu, H., Deng, J., Yang, Q., Zhang, R., Hu, Z., Liu, S., Sun, D., Peng, L., Wang, Y., 2022. Distinct cellulose nanofibrils generated for improved Pickering emulsions and lignocellulose-degradation enzyme secretion coupled with high bioethanol production in natural rice mutants. Green Chem. 24, 2975–2987.
Prusov, A.N., Prusova, S.M., Radugin, M.V., Bazanov, A.V., 2021. Flax shive as a source of activated carbon for adsorption of methylene blue. Fuller. Nanotub. Carbon Nanostructures 29, 685–694.
Si, S.L., Chen, Y., Fan, C.F., Hu, H.Z., Li, Y., Huang, J.F., Liao, H.F., Hao, B., Li, Q., Peng, L.C., Tu, Y.Y., 2015. Lignin extraction distinctively enhances biomass enzymatic saccharification in hemicelluloses-rich *Miscanthus* species under various alkali and acid pretreatments. Bioresour. Technol. 183, 248–254.
Tanaka, K., Murata, K., Yamazaki, M., Onosato, K., Miyao, A., Hirochika, H., 2003. Three distinct rice cellulose synthase catalytic subunit genes required for cellulose synthesis in the secondary wall. Plant Physiol. 133, 73–83.
Wang, Y.H., Srinivasakannan, C., Wang, H.H., Xue, G., Wang, L., Wang, X., Duan, X.H., 2022. Preparation of novel biochar containing graphene from waste bamboo with high methylene blue adsorption capacity. Diam. Relat. Mater. 125, 109034.
Wells, J.M., Drielak, E., Surendra, K.C., Kumar Khanal, S., 2020. Hot water pretreatment of lignocellulosic biomass: Modeling the effects of temperature, enzyme and biomass loadings on sugar yield. Bioresour. Technol. 300, 122593.
Wu, J., Yang, J.W., Feng, P., Huang, G.H., Xu, C.H., Lin, B.F., 2020. High-efficiency removal of dyes from wastewater by fully recycling litchi peel biochar. Chemosphere 246, 125734.
Xu, J., Dai, L., Gui, Y., Yuan, L., Ma, J., Zhang, C., 2020. Towards a waste-free biorefinery: A cascade valorization of bamboo for efficient fractionation, enzymatic hydrolysis and lithium-sulfur cathode. Ind. Crop. Prod. 149, 112364.
Yu, Y.L., Wan, Y., Shang, H.R., Wang, B., Zhang, P., Feng, Y.J., 2019. Corncob-to-xylose residue (CCXR) derived porous biochar as an excellent adsorbent to remove organic dyes from wastewater. Surf. Interface Anal. 51, 234–245.
Yu, J., Zhang, J., He, J., Liu, Z., Yu, Z., 2009. Combinations of mild physical or chemical pretreatment with biological pretreatment for enzymatic hydrolysis of rice hull. Bioresour. Technol. 100, 903–908.
Zakaria, M.R., Fujimoto, S., Hirata, S., Hassan, M.A., 2014. Ball milling pretreatment of oil palm biomass for enhancing enzymatic hydrolysis. Appl. Biochem. Biotechnol. 173, 1778–1789.
Zhang, R., Hu, H.Z., Wang, Y.M., Hu, Z., Ren, S.F., Li, J.Y., He, B.Y., Wang, Y.T., Xia, T., Chen, P., Xie, G.S., Peng, L.C., 2020a. A novel rice *fragile culm 24* mutant encodes a UDP-glucose epimerase that affects cell wall properties and photosynthesis. J. Exp. Bot. 71, 2956–2969.
Zhang, Y., Li, T., Shen, Y., Wang, L., Zhang, H., Qian, H., Qi, X., 2020b. Extrusion followed by ultrasound as a chemical-free pretreatment method to enhance enzymatic hydrolysis of rice hull for fermentable sugars production. Ind. Crop. Prod. 149, 112356.
Zhang, W., Yi, Z., Huang, J., Li, F., Hao, B., Li, M., Hong, S., Lv, Y., Sun, W., Ragauskas, A., Hu, Fan., Peng, J., Peng, L., 2013. Three lignocellulose features that distinctively affect biomass enzymatic digestibility under NaOH and H_2SO_4 pretreatments in *Miscanthus*. Bioresour. Technol. 130, 30–37.
Zheng, Y., Wang, J., Li, D., Liu, C., Lu, Y., Lin, X., Zheng, Z., 2021. Insight into the KOH/$KMnO_4$ activation mechanism of oxygen-enriched hierarchical porous biochar derived from biomass waste by in-situ pyrolysis for methylene blue enhanced adsorption. J. Anal. Appl. Pyrol. 158, 105269.